

# On Preempting Advanced Persistent Threats Using Probabilistic Graphical Models

Phuong Cao

University of Illinois at Urbana-Champaign

**Abstract**—This paper presents PULSAR, a framework for preempting Advanced Persistent Threats (APTs). PULSAR employs a probabilistic graphical model (specifically a Factor Graph) to infer the time evolution of an attack based on observed security events at runtime. The framework (i) learns the statistical significance of patterns of events from past attacks; (ii) composes these patterns into FGs to capture the progression of the attack; and (iii) decides on preemptive actions. The accuracy of our approach and its performance are evaluated in three experiments at SystemX: (i) a study with a dataset containing 120 successful APTs over the past 10 years (PULSAR accurately identifies 91.7%); (ii) replaying of a set of ten unseen APTs (PULSAR stops 8 out of 10 replayed attacks before system integrity violation, and all ten before data exfiltration); and (iii) a production deployment of the framework (during a month-long deployment, PULSAR took an average of one second to make a decision).

**Index Terms**—Factor Graphs, Attack Preemption

## I. INTRODUCTION

*Advanced Persistent Threats* (APTs) are among the most sophisticated attacks targeting networked systems [1]. Instead of exploiting a single vulnerability, an APT consists of several stages: an attacker (i) gains unauthorized access to a network, (ii) uses multiple attack vectors to pursue objectives repeatedly [2]–[4], and (iii) remains undetected for extended periods of time by staying under the radar of monitors [5]. Network and host security monitors [6] generate security events in APTs that often overlap with legitimate user activities. These result in high false positive rates (FPR) [7], [8] by threat detection software (TDS) [9] and security information and event management tools (SIEM) [10].

Despite the deployment of TDS/SIEM in large networks, successful attacks occur because security events by themselves (particularly if considered in isolation) are not sufficient indicators of malicious behavior or its progression. Often, system integrity has already been compromised (e.g., a rootkit is already installed) or data have been exfiltrated [11], [12] by the time a critical event occurs. Today, such critical events can only be handled by a nimble team of experienced analysts [13] using forensics and provenance tools [14], [15] among others. While these tools are useful, analysts still rely on their domain knowledge and learned (based on past security incidents) data characteristics (e.g., repetitiveness, severity, and common patterns of events) together, with the ongoing observation of events to investigate or respond to attacks.

The goal of this paper is to preemptively stop APTs with minimal false positives and low performance overhead. We use machine learning to fuse domain knowledge, experience of past attacks, and real-time observations from security monitors to detect and preempt an ongoing attack. We demonstrate this approach (PULSAR) in a production environment with real data from a large-scale, high-performance computing infrastructure that has thousands of nodes and both academic and industrial

users (anonymized under the name SystemX). The specific approach is based on probabilistic graphical models (PGM), particularly Factor Graphs (FG). The probabilistic nature of the model captures the uncertainty in (a) handling incomplete data and, (b) handling the significance of an event under different circumstances (as shown in §IV). In addition, FGs allow us (i) to capture temporal relationships among observed events, (ii) to build compositional models from the captured relationships to allow for machine interpretability, and (iii) to use the above information to form scalable real-time inference strategies so as to preempt attacks. We assert that FGs are a suitable formulation for modeling security attacks, because FGs model conditional dependencies and provide mechanisms to incorporate domain knowledge, while operating on modest data sizes (e.g.,  $N = 120$  attacks in this paper) with class imbalance. FGs are suitable for security analysis because successful attacks are rare (e.g., they represent only 0.01% of events in SystemX’s daily operation). An important benefit of FGs in contrast to provenance models [14], [15] is that relationships between sequences of security events and attack stages can be modeled statistically from historical data, and no assumptions are made about the causal ordering among events.

**Contributions.** The key contributions of this paper are: (i) An FG to model the progress of APTs targeting networked systems with thousands of nodes. (ii) A method to learn FG from annotated real-world attacks in which 99.7% of the data is annotated automatically. (iii) A testbed for testing ten attacks unseen at SystemX in the presence of legitimate traffic. (iv) A comprehensive runtime and accuracy evaluation.

**Evaluation.** We demonstrate PULSAR’s accuracy and performance via three experiments. *First*, we evaluated PULSAR on 120 real APTs observed in the past 10 years at SystemX. The dataset contains a variety of APTs that use different types of attack vectors, exploits, and payloads. When we trained PULSAR on one half of the historical attacks (60 out of 120 APTs) and tested it on the other half, PULSAR accurately identified 91.7% APTs prior to data loss. *Second*, to test its generalizability, we trained PULSAR on the entire historical dataset of 120 known APTs and tested it on ten APTs, unseen at SystemX. The unseen APTs, described in Table IV, are based on top ten attack techniques described in the IBM Threat Intelligence Index [2]. In order to have realistic attack scenarios, the unseen APTs were injected into live traffic where background events intermingled with attack events. PULSAR successfully stopped eight out of the ten unseen APTs before system integrity violation and all the APTs before data loss. *Third*, PULSAR was integrated into SystemX’s security infrastructure for a month-long deployment. During this period, there were an average of 94,238 events per day. PULSAR filtered this stream of events to an average of

**Table I:** Listing of attack stages  $\sigma_i \in \mathcal{S}$ .

Stage	Name	Description/Example
$\sigma_0$	Benign	Legitimate uses of the target system
$\sigma_1$	Discovery	Scan for open ports or applications
$\sigma_2$	Initial Access	Remote login into the target system
$\sigma_3$	Gathering	Reading kernel version
$\sigma_4$	Command & Control	Receiving attacker commands
$\sigma_5$	Preparation	Obtaining and compiling exploits
$\sigma_6$	Persistence	Installation of backdoor
$\sigma_7$	Lateral Movement	Accessing internal hosts
$\sigma_8$	Defense Evasion	Purging attack traces
$\sigma_9$	Collection	Recording secret keys or passwords
$\sigma_{10}$	Exfiltration	Using covert channels to extract secrets

1,885 significant events that it performed inference on at an average rate of one second per event.

**Putting PULSAR in Perspective.** While traditional SIEMs can output events of related attack vectors, such events often overwhelm security analysts [15]–[18]. Anomaly-based techniques (e.g., [19]–[21]) have potential to capture novel APTs, but they require extensive observations of normal usage profiles to detect anomalous activities, and also need substantial tuning to minimize FPR. Recent provenance-based techniques [15], [22] aim to build dependency graphs of APTs, however, these techniques require a complete causal observation of an APT and may be more suitable for offline analysis [14]. Our approach is unique in that i) it makes no assumptions about the causal ordering among events, and ii) it is trained and validated on both longitudinal and live production traffic.

## II. OVERVIEW

### A. Preliminaries

**Definition 1.** A *security event* (also referred to as an event)  $e_t \in \mathcal{E}$  is a variable that represents an observation of a potentially malicious activity at a time  $t$  using one or more security-related log messages from a TDS/SIEM. The set  $\mathcal{E} = \{\epsilon_1, \dots, \epsilon_m\}$  contains 105 possible values of events indicating APT activities found in both SystemX and other similar systems [23].

**Definition 2.** An *attack stage*  $s_t \in \mathcal{S}$  represents the progression of an APT at time  $t$ . The set  $\mathcal{S} = \{\sigma_0, \dots, \sigma_{n-1}\}$  contains  $n$  possible values of attack stages. This paper adopts the MITRE classification [3] that defines  $n = 11$  stages (see Table I) commonly found in APTs in the wild. Publicly disclosed APTs [5] follow these attack stages and have been used in prior work on APTs [22].

### B. Severity, Repetitiveness & Commonality

The key challenge for a security analyst is to identify an event or a set of events that are good indicators of an APT before it has caused any damage. To characterize known APTs, we analyze a longitudinal dataset (2008–present) of 120 security incidents at SystemX. Our dataset includes (i) human-written incident reports that indicate the users and the machines involved in the incident, (ii) raw logs of both legitimate user activities and attack activities, i.e., network flows (generated by a cluster of Bro network security monitors (NSM) [6]), system logs (generated by rsyslog, osquery, and ossec [10]), and (iii) audit logs of system calls (generated by auditd). These raw logs contain detailed attack activities. For each log message, we wrote scripts to remove specific (e.g., personal information [24], [25] or IP addresses) and non-deterministic information (e.g., time) and keep only the event in  $\mathcal{E}$  in the form of a symbolic

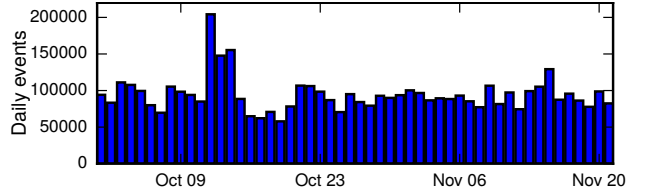


**Figure 1:** SystemX’s monitors observe an average of 94,238 events per day (standard deviation = 23,547) in Oct–Nov 2018.

name. For example, `download_sensitive` denotes a download of a file with a sensitive extension, e.g., `.c`, from an arbitrary node at any time. We assert that our dataset captures variants of known APTs and generalizes to unseen APTs (see §V).

In our dataset of 235K events, a majority of events (99.7%) have been automatically annotated with corresponding attack stages. These events are clearly benign (e.g., `login`) or clearly malicious (e.g., `installation of a binary file in an existing malware database`). Only a small fraction (0.3%) of events (i.e., ones that appear in both attack and legitimate activities) cannot be annotated automatically. We consulted with several security experts to annotate the remaining events. While we assume that the annotations by security experts are correct, i.e., attack events are labeled as malicious, we can reuse a body of work in ML that addresses annotation accuracy [26], [27]. Below we discuss the main characteristics of our dataset on APTs.

**Severity.** *Severe events* can be used to detect successful APTs; however, they cannot be used to preempt attacks because their occurrences indicate that the system integrity has already been compromised and that data have already been exfiltrated [28]. In fact, the entire dataset has 19 such unique critical events which occur 98 times in the 120 APTs. In all cases those critical events were detected when it was too late to preempt the system integrity loss. On the other hand, if any of events was considered as an indicator of a complete APT then analysts would have to analyze all of low- and medium-severity events (e.g., 94K daily events observed at SystemX in Fig. 1).

**Commonality.** Another way of identifying APTs is to look at characteristics shared by already known and new APTs, e.g., the longest common subsequence (LCS) [29] of events that lead up to malicious activity. For example, in Fig. 2a, we observe that 95% of the attacks in our dataset share at most 33.3% of their events. These events correspond to common attack vectors for establishing a foothold in the target network before executing exploits to exfiltrate secrets. Fig. 2b shows the histogram of 45 LCS (S1–S45) identified in our dataset. The histogram indicates that LCSs have common patterns across multiple attacks - which can be learnt.

**Repetitiveness.** APTs observed in our dataset (and in the wild [5]) often start with a set of *repetitive* but *inconclusive* events to identify vulnerable computing resources (e.g., scans for vulnerable Apache Struts portals [11]). Such repeated events are themselves not indicators of malicious activity, but can be used to signal potentially malicious events that need further monitoring. SystemX observes an average of 80k (out of 94K in Fig. 1) repeated port and vulnerability scans on a daily basis.

To summarize, use of individual events categorized by only one of the three data characteristics (i.e., severity, commonality, or repetitiveness) can detect the presence of an APT, but with two caveats: (i) the APT is already successful (i.e., the system

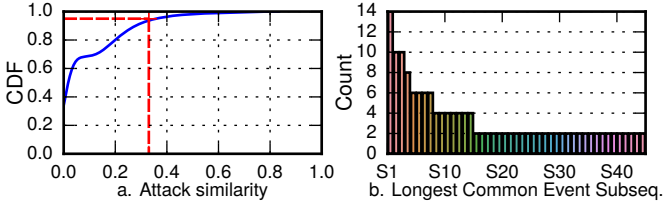


**Figure 2:** (a) The fractions of similar events between pairs of APTs in our dataset. (b) The count of LCS in our dataset.

integrity is already lost), or (ii) the FPR is high. We find, in the historical data at SystemX, that using events categorized by a single data characteristic can only detect 44% (53 out of 120) past APTs. Moreover, using individual events resulted in a high FPR of 87% when using only repetitive events as indicators of APTs as shown in Fig. 3.

**Proposition.** *We assert that combining events from diverse monitors with different characteristics and jointly analyzing (fusing) their statistical significance (likelihood of belonging to an attack) can lead to a more accurate APT detector that can effectively preempt attacks.*

We show how PULSAR works with a sophisticated attack.

### C. Motivating Example: The Attack

The Equifax attack (i) used a remote execution exploit (RCE) (publicly disclosed as CVE-2017-5638 [30]) to gain access; (ii) stayed undiscovered in Equifax’s system for an extended period of time [11]; (iii) extracted 143M Social Security Numbers. The goal of the attack was to get a shell (terminal) to control the Struts server without compromising a user’s account. While the CVE of the remote exploit is publicly known, we do not have the specifics of steps (ii) and (iii). In our attack, we used (i) a remote code execution exploit targeting Apache Struts (CVE-2017-5638, identical to the vulnerability in the Equifax breach), (ii) a privilege escalation (PE) exploit [31], (iii) a rootkit that uses port-knocking for stealthy data extraction using a DNS tunnel. To simulate the attack, we collaborated with SystemX’s redteam to setup a vulnerable Struts server in a virtual machine located in a production cluster at SystemX and launch the attack (i.e., via the RCE) from outside of SystemX. We collaborated with the SystemX analysts to analyze the event streams so as to understand their thought process.

While most APTs can take days to run, it would have been impractical for our attack to disrupt SystemX’s production systems for an extended period of time. Thus, we ran the attack for 10 minutes in a 24-hour period while production workloads were also running. SystemX’s security analysts did not know the exact time of the attack. While SystemX’s security team had a range of security analysis and forensic tools to assist in their investigation, they had to analyze events observed from host and network security monitors: on that day a total of 97,327 events were observed (black vertical bars in Fig. 4b; some are omitted for simplicity) out of which only 15 events (shown as colored bars) were related to the attack. The progression of our attack is depicted in Fig. 4a. The diamonds, ovals, and rectangles depict IP addresses, processes, and files, respectively. The attack progressed as follows.

In the *discovery stage*, the attack *repetitively* scanned for vulnerable Apache Struts portals (i.e.,  $\epsilon_1, \dots, \epsilon_4$ ) in Fig. 4b.

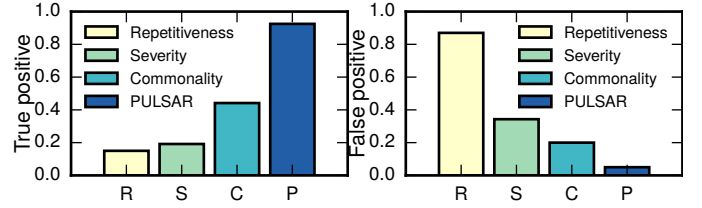


**Figure 3:** Combination of multiple events (using PULSAR) provides more accurate detection.

Those scan events did not require immediate action from SystemX’s operators because a few scans do not lead to network congestion, and hence such activities were considered routine. Once a vulnerable Struts server is identified, the attack gained initial access by exploiting the remote code execution vulnerability (i.e.,  $\epsilon_5$ ) that blends into scan events.

The *gathering stage* in Fig. 4a illustrates each of the attacker’s actions with its corresponding UNIX command. In order to make sure that the system admin was not present, the attack queried currently active users (i.e.,  $\epsilon_6$ : command `w`). The attack obtained the kernel version to prepare for a suitable exploit (event  $\epsilon_7$ , command `uname`). In the *preparation stage*, the attacker established a reverse shell to his/her machine and transferred the source code of the PE exploit (`cowroot.c`) and a sophisticated rootkit (`knockd.c`) to the legacy memory-mounted disk (`/dev/shm`; i.e.,  $\epsilon_8$ ) to make sure that no attack traces would be presented on the disk file system.

In the *privilege escalation stage*, the attacker obtained a compiler toolchain ( $\epsilon_9$ : command `apt`) and compiled ( $\epsilon_{10}$ : command `cc`) the exploit. Unlike Windows environments in which malicious binaries can run directly, SystemX uses a variety of highly customized Linux distributions for different computing tasks. Thus, attackers could not deploy binaries directly even if they got the kernel version. In our past APTs, attackers must compile exploit code for the specific kernel configuration of the target machine. After executing the compiled PE exploit, the attacker became the superuser: this activity corresponded to a severe event (i.e.,  $\epsilon_{11}$ ). If the attack was not stopped here, the attacker could compile the rootkit and load (`insmod`) the rootkit as a kernel module (i.e.,  $\epsilon_{12}$ ).

In the *persistence stage*, once the kernel module (`knockd.ko`) has been loaded, the attacker could maintain *persistent* access by using two rootkit components: (i) a user-level backdoor that listens at port 9090 to receive remote commands, and (ii) a net-filter kernel hook that provides a stealth *port-knocking service* for the user-level backdoor, i.e., the port only opens for a short period of time upon receiving a specific “knocking” sequence of three TCP packets such that `src_port + seq_number = 1221`. Thus, the secret port stays under the radar of network-security scanning tools (which treat these packets as misrouted or corrupted). Finally, in the *exfiltration stage*, the attacker extracts secret SSH keys (`id_rsa`) and data (`portal.db`) by using a DNS tunnel (`iodine`; i.e.,  $\epsilon_{13}, \dots, \epsilon_{15}$ ).

### D. Motivating Example: The Defense

We describe the defense from the perspective of an experienced security analyst and show how PULSAR uses machine learning to automate the detection process.

Assuming that an analyst observes a stream of events (see Fig. 4), we expect that s/he will focus on three key events. First,



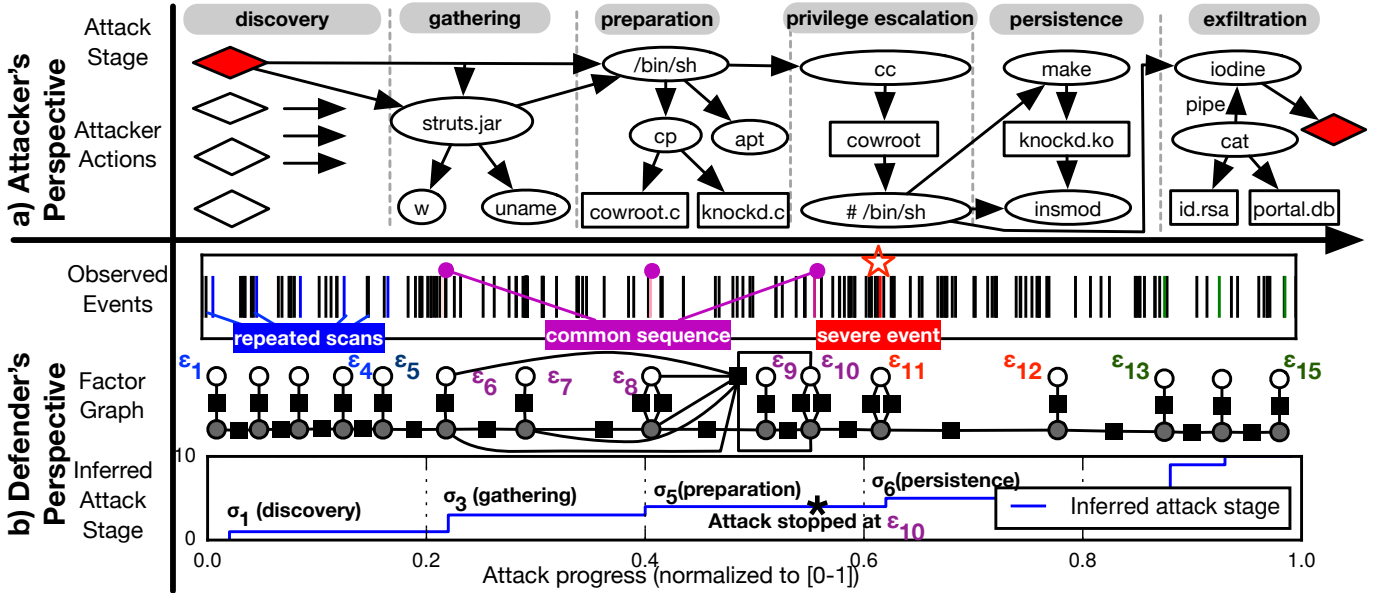


**Figure 4:** (a) Attacker's view of the exercised APT. (b) Defender's view of detected attack stages and recommended actions.

on observing scans  $\epsilon_1 - \epsilon_4$ , the analyst might suspect malicious intent, but have low confidence that it might mature into an attack (a few scans seldom lead to a major attack). Second, the system queries  $\epsilon_6, \epsilon_7$  increase the analyst's suspicion. Most benign users do not query detailed system configurations (although they might). At this stage, the analyst's confidence increases, but not enough to warrant a reaction. As a result, the decision is to continue to monitor additional events. The third set of key events is the placement and compilation of the source file in the memory-mounted disk, i.e.,  $\epsilon_8, \epsilon_9, \epsilon_{10}$ . Although these events may be used in legitimate activity to speed up I/O (e.g., an in-memory file system),  $\epsilon_8$  is also observed in attacks, as such volatile storage does not leave any forensic evidence after system reboot. Finally, the analyst observes  $\epsilon_{11}$ , a *severe* event corresponding to PE. If the attack is not stopped at this point, the system integrity will be lost, i.e., the attacker will get superuser permission. However, one must note that PE is not always a malicious event. In some contexts (especially on personal workstations on enterprise networks) ordinary users might have legitimate reasons to escalate to a superuser, e.g., to perform an operating system upgrade.

The above scenario assumes there is an experienced analyst who can analyze the events in a stream, presumably with the help of various tools, to make a decision. However, performing such an analysis in real-time today is generally impossible, as there are an average of 94K events per day. Note that our hypothetical analyst made his/her decision based on (i) *repetition* of scans, (ii) *commonality* of the action (since observed previous incidents involved system configuration queries), and (iii) *severe-critical* use of the compilation of the source code on the volatile file system. In addition, taken together, the sequence of a *scan*, followed by *system configuration queries*, and the *placement and compilation* (of source files) in a memory-mounted disk, is one of the 45 common event sequences in our dataset (see Fig. 2).

We present in this paper a machine-learning based approach, based on PGM [32]–[38], which builds an FG [33] for each user, and can perform real-time detection. Our approach learns

from past events to build prior knowledge and uses the learned domain knowledge of the system together with observed runtime events. PULSAR can achieve this in the presence of noisy events, i.e., many users using the system. As each event is observed, PULSAR adds a factor function (FF) to the event that characterizes its commonality, severity, or repetitiveness. These factor functions are learned by extracting events sequences from our dataset of 120 past APTs. At its core, an FF captures how frequently is an event (or an event sequence) occurred in past APTs and the statistical significance. The FFs together with observed events, are used to infer attack stages, which allows our decision algorithm to preemptively stop an attack.

PULSAR processes events as follows. First, each of the scan events  $\epsilon_1 - \epsilon_4$  has an FF attached to it to capture the frequency and the significance of repetitive scans. This FF indicates that the attack has not yet met the stopping threshold (i.e., the attacker is only discovering the system). Then, the attacker gets a terminal to control the Struts server (event  $\epsilon_5$ ). After that, when PULSAR observes the events *query active users* and *query kernel version*  $\epsilon_6, \epsilon_7$ , it adds FFs to the event to capture these events severity. The FFs indicate that the events are not severe, and thus the attack continues to be monitored. If any observation of this event was stopped, many legitimate users would be unable to work. Finally, PULSAR observes the placement and compilation of source code, i.e.,  $\epsilon_8 - \epsilon_{10}$ , which combined with past events ( $\epsilon_6, \epsilon_8, \epsilon_{10}$ ) forms a common sequence. While individual events in this sequence can be legitimate, the whole sequence has occurred frequently in past APTs. Now, PULSAR outputs the attack stage as preparation (immediately before PE) and notifies analysts to stop the attack.

We quantify PULSAR's preemptive detection capabilities in terms of: i) *preemption before system integrity violation and before data loss* and ii) *preemption after system integrity violation (SI) but before data loss (DL)*. These metrics can be quantified in terms of the distance (in hops) calculated by a function  $\text{hop}(D_\sigma, L_{\text{SI+DL}})$  between  $D_\sigma$ , the stage when an attack is detected (i.e., *stop* action is suggested), and  $L_{\text{SI+DL}}$ , the actual system integrity violation without any data loss. This

hop-based metric is time-independent; thus, it can characterize attacks that happen on various time-scales, e.g., on the order of minutes, days, or weeks. PULSAR stops the 6-stage APT above (Fig. 4) at its 3<sup>rd</sup> stage, i.e., at  $D_\sigma = \sigma_5$  (preparation), while the system integrity violation is at  $L_{SI+DL} = \sigma_6$  and  $\text{hop}(D_\sigma, L_{SI+DL}) = 1$ . Fig. 4b shows that PULSAR infers attack stages that approach the successful completion of the APT. Finally, PULSAR’s decision is presented to security analysts. These decisions could be automated by actuators, e.g., which could redirect malicious network flows [39]–[42] or allocate resources for further monitoring [43].

### III. THREAT MODEL AND ASSUMPTIONS

**Target system.** This paper considers multiuser, multinode, networked computer systems that provide computational services in which users remotely execute workloads on internal hosts (physical/virtual machines). The system is assumed to be benign at the onset. The system may have unpatched vulnerabilities due to the complexity of patching highly interconnected system components. Indeed, recent surveys [44], [45] found that 37% of the top 133k websites still use vulnerable libraries.

We assume that the events from network- and kernel-based monitors are trustworthy [46]–[55] and accurate in capturing attack activities. Since our approach’s accuracy depends on monitors, we use an extensive set of well-configured (e.g., SystemX uses a Bro cluster for network monitoring) and well-protected monitors (e.g., osquery runs at the kernel-level). While an attacker may tamper with one monitor (on one host) by using the credential of a local privilege user, it would be challenging to manipulate *all* monitors. We describe an example attack (A2 in §V) that manipulates the Bro cluster to suppress attack-related security events; however, PULSAR still works.

**Attacker Capabilities.** This paper assumes that an attacker can pretend to be a legitimate user by using weak/stolen credentials [56]–[59] or remote command execution exploits [30] to compromise internal hosts. PULSAR treats it as a single attack if (1) an attacker moves laterally (e.g., connects by SSH to multiple machines) using the same user account and (2) multiple (coordinated or independent) attackers launch an attack using the same user account. If (1) an attacker moves laterally using different user accounts, or (2) one or more attackers use different entry points and launch attacks using different user accounts, PULSAR treats that as multiple separate attacks.

An attacker may mimic legitimate user activities [60] to obfuscate attack-related activities. Such an attack only works against TDSs that use a small sliding window of events (e.g., 9 events in [61]) to detect an attack. PULSAR uses a larger sliding window of 10,000 events, and filters insignificant events (§V). If an attacker fills up PULSAR’s sliding window, PULSAR will not be able to detect the attack. However, such attack activities might cause significant perturbations in system operations, and hence be observable to the operators.

The boundary of our threat model is that PULSAR cannot preempt an attack if the attacker (e.g., a malicious insider) executes an attack (i) in a single step without being persistent, (ii) with no time evolution involving prior events, and (iii) without events in common with any of the past APTs. Nonetheless, as we showed in our results, our threat model can capture a wide variety of attacks, as discussed in §VI.

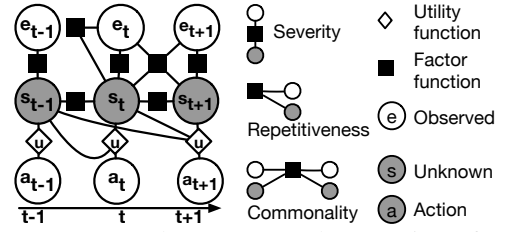


Figure 5: An example Factor Graph at runtime (from §IV).

### IV. LEARNING AND INFERENCE MODEL

This section introduces FGs and demonstrates its advantages in addressing the threat model.

#### A. Formulating APT Defence as a FG

**Definition 3.** A *Factor Graph* [33] is a graphical representation of the factor-argument dependencies of a real valued function. Given the factorization of a function  $f(x_1, \dots, x_n)$ ,

$$f(x_1, \dots, x_n) = \frac{1}{Z} \prod_{i=1}^m f_i(X_i), \text{ where } X_i \subseteq \{x_1, \dots, x_n\}$$

The corresponding FG  $G(X \cup F, A)$  is a bipartite graph that consists of variable vertices  $X = \{x_1, \dots, x_n\}$ , factor vertices  $F = \{f_1, \dots, f_m\}$ , and arcs  $A = \{(x_i, f_j) \mid x_i \in X_j\}$ . The functions  $f_i$  are called *factor functions*.

**Definition 4.** An *event timeline* is a sequence of events  $E_t = \{e_i \mid i \in [0, t]\}$ , observed at each time step  $i$  until the time  $t$ . We also call such a timeline an *event stream*.

**Definition 5.** A *attack-stage timeline* is a sequence of unknown stages  $S_t = \{s_i \mid i \in [0, t]\}$  corresponding to  $E_t$ .

PULSAR uses the FG formulation (shown in Fig. 5) to describe the progression of APT by factorizing the joint probability distribution (pdf) of  $E_t$  and  $S_t$  as

$$P(E_t, S_t) = \frac{1}{Z} \prod_c f_c(X_c), \quad (1)$$

where  $Z$  is a normalization factor that ensures  $P$  is probability distribution. Each set of random variables  $X_c$  contains a subset of events  $E_c$  and attack stages  $S_c$  such that  $E_t \cup S_t = \bigcup_c (E_c \cup S_c)$ . §IV-B will describe how the attack characteristics (from §II-B) of *severity*, *commonality* and *repetitiveness* can be encoded into FFs and the choice of different  $X_c$ . The PULSAR FG makes no assumptions about the causal ordering among events. This is a fundamental strength of PULSAR compared to other techniques like provenance techniques [14] as it is difficult to define the causal ordering of events in realistic attacks.

#### B. Formulating & Training Factor Functions

The challenges with formulating the FFs for the FG described above (from (1)) are (a) to find the set  $X_c$  by selecting events from  $E_t$  and states from  $S_t$ ; and (b) to find a functional form of  $f_c$  that relates the variables in  $X_c$ . PULSAR’s definition of FFs presents a three-fold solution to the challenges above, i.e., it uses the three common characteristics (from §II-B) of the attacker actions (behavior) observed in past attacks as three separate class of FFs. Each attack behavior is represented by a set of events and its corresponding attack stages as its input (i.e.,  $E_c$  and  $S_c$  above). Although these variables define a large combinatorial space, PULSAR focuses only on observations that are (a) highly frequent in a past attack, and (b) statistically significant, so that the observation reliably indicates an attack.

We capture the frequency of a sequence of events  $E_c$  and attack-stages  $S_c$  in a function  $q(E_c, S_c)$  such that

$$q(E_c, S_c) = \begin{cases} P(E_c, S_c), & \text{if } E_c \text{ is obs. in the cur. attack} \\ 0, & \text{otherwise} \end{cases} \quad (2)$$

where  $P(E_c, S_c)$  is the probability of observing  $E_c$  having states  $S_c$  in the training dataset  $\mathcal{D}$ . We capture the statistical significance of the event- and attack-stage-sequence by computing the significance level  $p(E_c, S_c)$  (i.e.,  $p$ -value: the probability that the null-hypothesis is *true*) of observing  $E_c, S_c$  under the null-hypothesis that “the target system is currently not under attack”. To combine both frequent and significant characteristics, PULSAR uses exponential form FFs, i.e.,

$$f(E_c, S_c) = \exp\{q(E_c, S_c)(1 - p(E_c, S_c))\}. \quad (3)$$

The advantages of this exponential form are that (a) it achieves numerical stability for small values of  $q(X_c)$  and  $p(X_c)$  (especially when attacks are rare events), and (b) it ensures that the product of FFs is a convex function. Convex-exponential FFs allow us to efficiently optimize the joint pdf in our learning and inference steps by using the *log-sum-exp* trick. For notational simplification, we use the shorthand  $p_c = p(E_c, S_c)$  and  $q_c = q(E_c, S_c)$ .

PULSAR maps the problem of learning FFs into finding the parameters  $p_c$  using patterns from past security incidents to capture three characteristics of APTs: *commonality*, *severity*, and *repetitiveness*. PULSAR utilizes an ensemble of generic statistical hypothesis testing frameworks [62], each of which is customized for the properties mentioned above. Only the FFs which have a high significance ( $p_c \leq 0.05$ ), i.e., that observing the properties under the null hypothesis is unlikely) are considered for use in (1).

The FFs are trained from an annotated dataset of past attacks  $\mathcal{D} = \{A_i \mapsto [E_i^t, S_i^t, U_i^t] \mid \forall i\}$  which consists of a set of attacks  $A_i$ , each of which includes an event timeline  $E_i^t$ , an annotated attack stage timeline  $S_i^t$ , and an ownership map  $U_i^t = \{u_j \mid j \in [0, t] \wedge u_j \text{ owns } e_j \text{ in } E_i^t\}$  which identifies which user is responsible for which event. In addition, we have a list  $\mathcal{U}$  which identifies the malicious users in each scenario. Using this formalism of the input dataset, we consider the training procedure of each of the FFs presented above as follows.

**The Severity FF.** Severity FFs measure the maliciousness of an event. We consider an event malicious when an attacker has taken control of the system or has caused significant damage. It can be argued that traditional signature-based TDS (e.g., [6]) are a degenerate (non-probabilistic) case of the severity FF. Hence, in the case of severity FFs,  $E_c = \{e\}$  and  $S_c = \{s\}$ . To understand the occurrence of an event  $e$  in  $\mathcal{D}$  we compute two probabilities  $P_{A,s}(e)$ , the probability of an event being from attack stage  $s$ , and  $P_B(e)$ , the probability of an event being benign. So

$$p_{\text{Severity}}(e, s) = \chi^2 \left( \left\{ \frac{P_{A,s}(e)}{\sum_x P_{A,s}(x) + P_B(x)}, \frac{\sum_x P_{A,s}(x) - P_{A,s}(e)}{\sum_x P_{A,s}(x) + P_B(x)} \right\}, \left\{ \frac{P_B(e)}{\sum_x P_{A,s}(x) + P_B(x)}, \frac{\sum_x P_B(x) - P_B(e)}{\sum_x P_{A,s}(x) + P_B(x)} \right\} \right), \quad (4)$$

where  $\chi^2(\cdot)$  represents the  $p$ -value of the chi-squared test [62]. This test is applicable for testing dependencies of categorical

variables, i.e., dependency between the observed events and the attack stage. In the training phase, the value of  $p(e, s)$  for all statistically significant combinations of  $e$  and  $s$  is computed offline and stored for use at inference.

**The Commonality FF.** Commonality FFs measure the similarity between a sequence of events observed during an attack and all past known attacks. Thus, conventional similarity measures, such as Hamming distance or string similarity, are not suitable. To capture the aforementioned characteristics, we quantify similarity using the longest common subsequence (LCS) measure [29], [63] which outputs a sequence of events that appear in the same order in two attacks. This LCS approach works with mimicry attacks in which attackers inject arbitrary noise to the event sequence. Note that attackers may not simply change the order of events to trick our approach, because many events depend on each other, e.g., executing the binary file of a memory exploit first requires the successful compilation of the exploit from the source code.

In the training phase, the LCS  $L_{i,j}$  is computed for all pairs  $(A_i, A_j)$  (such that  $i \neq j$ ) of attacks in  $\mathcal{D}$ . Each unique value of  $L_{i,j}$  has an annotated attack stage  $S_{i,j}$ . The commonality FF's  $p_c$  is calculated as

$$p_{\text{Common}}(L_{i,j}, S_{i,j}) = \mathbb{F} \left( \left\{ \frac{P_{A,S_{i,j}}(L_{i,j})}{\sum_x P_{A,S_{i,j}}(x) + P_B(x)}, \frac{\sum_x P_{A,S_{i,j}}(x) - P_{A,S_{i,j}}(L_{i,j})}{\sum_x P_{A,S_{i,j}}(x) + P_B(x)} \right\}, \left\{ \frac{P_B(L_{i,j})}{\sum_x P_{A,S_{i,j}}(x) + P_B(x)}, \frac{\sum_x P_B(x) - P_B(L_{i,j})}{\sum_x P_{A,S_{i,j}}(x) + P_B(x)} \right\} \right), \quad (5)$$

where  $\mathbb{F}(\cdot)$  is the  $p$ -value of the Fisher exact test [62] and  $P_{A,S_{i,j}}$  and  $P_B$  are defined as above. We test for significance of the LCS by using this test on a small sample size, e.g., a limited observation of attacks, as malicious attacks are rare compared to legitimate activities in our data source. All statistically significant combinations of  $L_{i,j}$ ,  $S_{i,j}$  and  $p(L_{i,j}, S_{i,j})$  are stored for use at inference.

**The Repetitiveness FF.** A repetitiveness FF measures the periodicity of an event. Regular events occurring in a regular period are often results of the repeated execution [64] of automated scripts and hence can be used as an indicator of automated attacks at an early stage (e.g., periodic port scan events [65], [66]).

For every event  $e$  which is annotated with attack stage  $s$  in an attack  $A_i$ , PULSAR computes a the frequency  $H_{s,e,n,k}^{(i)}$  of occurrence (i.e., number of repetitions) of  $(e, s)$  in the time interval  $[nk, (n+1)k]$  during the attack  $A_i$ . Then

$$p_{\text{Repetitive}}(e, s) = \min_{i,n,k} \text{DW} \left( \left\{ H_{s,e,n,k}^{(i)} \mid A_i \in \mathcal{D} \right\} \right), \quad (6)$$

where  $\text{DW}(\cdot)$  is the  $p$ -value of the Durbin-Watson test [62]. These DW tests are computed in training. The statistically significant repetitive events are stored for use in inference.

All three FFs above are generated by statistical tests based on the counts of past events. Thus, when a new attack is observed, PULSAR does not need to re-learn the FFs. Instead, it increments the frequency of the events sequences (according to the events in the new attack) and reruns the statistical tests above. This notion of incremental training proposition is useful



**Algorithm 1: Construction and inference on FG**


---

**Input** : Set of learned factor functions  $F$ ,  
An event timeline  $E_t$  up to a time  $t$

**Output** : Sequence of attack stages  $\hat{s}_t$ ,  
Action  $\hat{a}_t \in \mathcal{A}$

```

1 FG  $\leftarrow \emptyset$ 
2  $\Delta \leftarrow 0.05$ 
3 for  $e_i \in E_t$  do
4   add an event node  $e_i$  to the FG
5   add an attack stage node  $s_i$  to the FG
6   add a transition FF between  $s_i$  and  $s_{i-1}$ 
7   for  $f \in F$  do
8     if  $q_f > 0$  and  $p_f \leq \Delta$  then           // select a ff
9       add the factor function  $f$  to the FG
10    end
11  end
12 end
13  $\hat{s}_t \leftarrow \text{TRW}(P(E_t, S_t))$            // using Tree Reweighted to find  $\text{argmax}_i$ 
14  $\hat{a}_t \leftarrow \text{argmax}_a \sum_{i \in S} P(\hat{s}_t = i) \times u(a, i)$ 
15 return  $(\hat{s}_t, \hat{a}_t)$ 

```

---

for systems that observe new attacks on a daily basis. For attacks that introduce new events, we discuss them in §VII.

**Constructing FGs.** At runtime, the FG only contains an event  $e_t$  and an unknown stage  $s_t$ . PULSAR selects FFs (from the learned FFs above) that are statistically significant and adds these FF to the FG to connect  $e_t$  and  $s_t$ . When a new event  $e_{t+1}$  is observed, the above procedure is repeated. In addition, PULSAR adds a transition FF:  $f(s_t, s_{t+1})$  that captures the probability that a stage  $s_t$  leads to a stage  $s_{t+1}$ . This probability is represented by a  $11 \times 11$  matrix. Finally, PULSAR performs inference on unknown attack stages.

### C. Inference On Factor Graphs

PULSAR uses the constructed FG above and its inference algorithm (see Algorithm 1) to predict the sequence of unknown attack stages  $S_t$  associated with a sequence of observed events  $E$  up to a time  $t$ . Based on how an analyst responds to an attack at SystemX, we consider a three-tiered decision model (see Table II) that separates actions from their implementations, which might be system dependent. Based on that estimate of  $S_t$ , a preemptive action  $a_t$  (e.g., *no-operation*, *monitor* a user closely—via deep packet inspection, or *stop* the user immediately) is suggested to an analyst.

PULSAR’s inference procedure finds the most probable attack stages that minimize the energy [67] of the FGs. Since our FG can have loops (two variables may be connected by more than one factor function), loopy BP does not guarantee convergence: the inferred attack stages may reach the global minimum energy of the FG. Therefore, we adopted the sequential tree-reweighted (TRW) message passing scheme [68] that: i) decomposes the loopy FG into smaller FGs without a loop, ii) guarantees that the inference procedure will converge. Using TRW, PULSAR infers a maximum likelihood estimate (MLE) for a sequence of *unknown* attack stages  $\hat{S}_t$  (up to time  $t$ ) associated with an event timeline  $E_t$ . Further, it outputs a confidence level for each stage, as an event is observed. That means finding  $\hat{S}_t = \text{argmax}_S P(E_t, S)$ , where  $P(E_t, S)$  is defined using the factorization equation (§IV) in FGs. The result of this optimization procedure is the most likely sequence of attack stages associated with observed events. This procedure provides the step-by-step estimate of attack stages for analysts.

**Table II:** List of preemptive actions in the PULSAR reward model (see Fig. 6).

Action	Description
$\alpha_1$	Benign user behavior, no immediate action needs to be performed.
$\alpha_2$	An attack may be in progress, and further monitoring is required.
$\alpha_3$	An attack is imminent and must be stopped immediately.

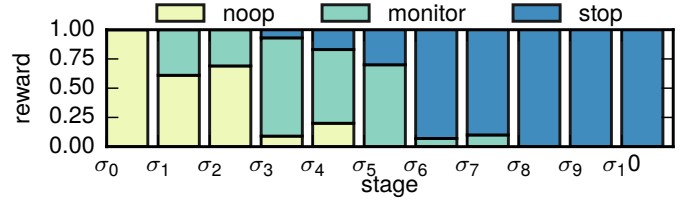


**Figure 6:** Reward function  $u(a, s)$  for each attack stage.

**Algorithm 2: Computing the reward function  $u(a, s)$ .**


---

**Input** : Training data  $D$  of size  $n \times 11$ ,  
Priors  $\mu_p = \{\mu_a | a \in \mathcal{A}\}$ , and  $\Sigma_p = \{\Sigma_a | a \in \mathcal{A}\}$

**Output** : Reward function  $u(a, s)$

*/\* Definition:  $\text{GMM}(x|k, \mu, \Sigma) = \sum_{i=1}^k w_i \times \mathcal{N}(x|\mu_i, \Sigma_i)$  \*/*

```

1  $w, \mu, \Sigma \leftarrow \text{EM}(D, k, \mu_p, \Sigma_p)$            // Train  $k=3$  GMM model
2  $u \leftarrow \emptyset$ 
3 for  $a \in \mathcal{A}$  do                                   // Corresponding to  $\{\alpha_1, \alpha_2, \alpha_3\}$ 
4   for  $s \in [0, 10]$  do                             // Corresponding to  $\{\sigma_0, \dots, \sigma_{10}\}$ 
5      $u(a, s) \leftarrow w_a \times \mathcal{N}(I_{11}[s, :], \mu_a, \Sigma_a)$ 
6   end
7 end
8 return  $u$ 

```

---

### D. Decision on maliciousness of an attack

The FG model is extended with “reward factor functions” to produce a decision model that determines an optimal action based on the inferred attack stage (see Fig. 5) to support learning [69]. The decision model has two new components: 1) a finite action space  $\mathcal{A} = \{\alpha_1, \alpha_2, \alpha_3\}$  (see Table II), and 2) a reward function  $u : \mathcal{A} \times S \rightarrow \mathbb{R}$ . The output of the decision model allows security analysts to closely track the progress of an ongoing attack and implement response strategies. The decision model is useful when PULSAR is not confident in its inferred attack stage (i.e., the prediction probability is close to 50%). In this case, a *monitor* action ( $\alpha_2$ ) is recommended instead of immediately stopping user activity, which would otherwise lead to FPs. At time  $t$ , the decision model uses the inferred attack stage  $\hat{s}_t$ , and its probability  $P(\hat{s}_t)$ , to choose an action  $\hat{a}_t$  that maximizes the reward over  $P(\hat{s}_t)$  in §IV-D.

To model a mapping from attack stages (obtained from FG’s inference) to three actions that analysts at SystemX do, we use a 3-component Gaussian Mixture Model (GMM; corresponding to the 3 actions described in Table II) with priors to construct the reward functions. Gaussian has a conjugate prior distribution that augments these functions with operational information about past incidents, i.e., actions that SystemX’s security team has taken in past incidents. A reward function  $u(a, s)$  (see Fig. 6) on an action  $a$  being taken at stage  $s$  is estimated over a 11-D space (corresponding the attack stages  $\sigma_0, \dots, \sigma_{10}$ ). Each of the components (clusters) in the GMM corresponds to one of the actions  $\{\alpha_1, \alpha_2, \alpha_3\}$ . For example, in the early attack stages  $\sigma_0, \sigma_1$ , the no-op action  $\alpha_1$  is preferred. In the intermediate stages  $\sigma_2, \sigma_3$ , the monitor action  $\alpha_2$  (i.e., deep packet inspection) is preferred. Finally, in attack stages

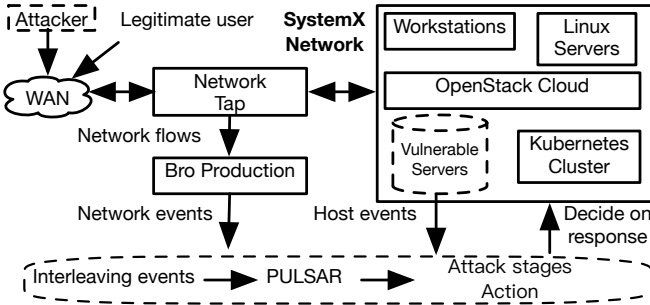


Figure 7: Testbest architecture for evaluating PULSAR.

Table III: Summary of dataset used in our experiments.

Description	Past	Unseen	Production
Total events	235K	1.25M	4.9M
Unique events	105	68	42
Number of APTs	120	10	–
Type of APTs	Known	Unseen	Attempted
Data duration	10 years	1 week	1 month

$\sigma_4, \dots, \sigma_{10}$ , the stop action  $\alpha_3$  has a higher reward than  $\alpha_1$  &  $\alpha_2$ . The training procedure (using *expectation maximization*) is described in §IV-D.

## V. EVALUATION SETUP

Real-world APTs blend their attack events with background activities of legitimate users running production workload. The question is whether PULSAR can identify real APTs in a timely manner. We demonstrate PULSAR’s accuracy and performance via three experiments. *First*, we evaluated PULSAR on 120 past APTs retrospectively. *Second*, we evaluated PULSAR’s detectability on ten unseen attacks constructed using the IBM Threat Intelligence Index and injected in live traffic where normal security events were intermingled with the unseen attack events. *Third*, PULSAR was integrated into SystemX’s security infrastructure, for a month-long trial, while measuring its performance overhead.

### Experiment 1: Evaluation based on successful past APTs.

To provide a baseline estimation of the accuracy of PULSAR in correctly detecting past APTs, data on 120 past APTs is divided into two disjoint sets: (i) a set of 60 attacks (2008–2009) for training PULSAR’s factor functions and (ii) a set of 60 attacks (2010–present) for evaluating PULSAR’s accuracy in detecting the past APTs<sup>1</sup>.

**Experiment 2: Evaluation based on APTs unseen at SystemX.** To test the efficacy of PULSAR in detecting attacks never observed in SystemX, we reconstructed and replayed ten attack scenarios (described in Table IV). For this, we studied the mechanisms of high-profile attacks [5], [70] (e.g., the Equifax data breach [11]) and reconstructed attack scenarios using top ten attack techniques from the IBM Threat Intelligence Index [2]. These attack scenarios use different techniques, such as local privilege escalation in A2, A8 and remote exploit in A1, A6; a custom rootkit in A1; a custom backdoor in A4; and custom exploits in A9, A10. None of these attacks have been observed in the past at SystemX.

The attack scenarios in Table IV represent major data breaches [11], credential stealing [70], and system integrity violations (e.g., escaping from the isolation mechanism of

<sup>1</sup>SystemX has observed fewer attacks in recent years than before 2010 because of improved security policies and authentication systems.

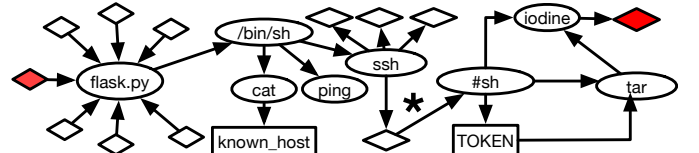


Figure 8: An example sophisticated scenario (A2) that uses a coordinated DDoS attack and an OAuth bypass exploit.

Linux containers). Thus, they show both the depth (in terms of sophistication) and the breath (in terms of the variety of techniques) of APTs. The attack scenarios were in live traffic during production workloads at SystemX; thus, it is not possible to precisely characterize the similarity between the scenarios and past APTs.

Because of space constraints, we describe just one sophisticated attack scenario (A2) that attempts to manipulate security monitors. In A2, the attacker ran a mimicry attack against a Python flask server that authenticates users using a vulnerable pysaml2 library (Fig. 8). To mislead security analysts and blend the real exploit into legitimate activities, the attacker attempted to flood Bro by launching hundreds of legitimate-looking requests to the flask server and other servers. In this case, Bro did not have a signature of the exploit (OAuth bypass [71]), and thus, allowed the attacker to access the vulnerable flask server. PULSAR, however, received the following events from Bro and the host monitors: i) intermittent packet capture losses while production workloads were not high; ii) accessing a list of internal hosts (known\_host file); and iii) unscheduled internal network scans. Combining above events, PULSAR recognized and stopped this attack at the lateral movement ( $\sigma_7$ ) in which the attacker was attempting to access other hosts.

Accurate reconstruction and replay of such attack scenarios, however, presents several challenges.

**Challenge 1.** The emulated attack scenarios must include background traffic (i.e., legitimate user activities and background noise such as legitimate port scans) in order to be realistic. Fig. 7 shows the experimental setup used to collect both types of traffic. Each attack scenario was setup in a vulnerable server (i.e., one that contained software with a known vulnerability) alongside SystemX’s workstations, servers, an OpenStack cloud, and a Kubernetes cluster. We simulated a remote attacker accessing the system through the WAN connection to exploit the vulnerable servers in the attack scenarios. Network flows in/out of SystemX (with an average of 12Gbps and a maximum of 40Gbps) were captured via a network tap device at the network border by a Bro cluster of 16 nodes to output network events. Host logs were captured via host-auditing tools and collected via rsyslog to output host events. Both host and network events were collected for preprocessing and analysis by PULSAR. The events were filtered into logical channels. Each channel was a stream of events that was associated with a user. PULSAR subscribed to each channel and constructed a per-user FG, and inferred attack stages/decisions at runtime.

**Challenge 2.** The volume of events generated by monitoring tools in the production system is quite significant and it is possible for attack events to be hidden in this large volume of events. Fig. 1 shows that the test environment experiences a daily average of 94,238 events for a total of 2,032 registered users (at peak times: no more than half of the users use the



**Table IV:** Ten representative APTs that use top-10 and representative attack vectors from the IBM Threat Intelligence Index [2].

ID	Name	Description	Common events with past attacks
A1	Port knocking	Exploit a remote code execution vulnerability CVE-2017-5638 in an Apache Struts web server and read a database of personal information.	Network scan, get kernel version, access mem disk, compile, new kernel module.
A2	DDoS and OAuth	Flood network monitors with a high-volume stream of benign-looking requests, forcing the monitor to drop packets. Concurrently, attackers exploit an auth. bypass bug CVE-2017-1000433 in the pysaml2 library to steal access tokens.	High network flows, packet loss, access known.host file, scan internal servers, excessive POST req.
A3	Container Escape	Exploit a heap vulnerability CVE-2017-5123 on a Kubernetes cluster to read SSH keys in hosted containers.	Get kernel version, compilation, access id_rsa file.
A4	SSH Keylogger	Deploy an SSH keylogger into an OpenSSH server, to record credentials of subsequent user logins.	Concurrent login, compilation, restart system service, unknown SSH client.
A5	Ransomware	Spread ransomware that uses CVE-2017-0144. The ransomware registers itself as a system service to scan for and steal secret files.	New sys. service, scan internal SMB servers, transfer .exe files via SMB.
A6	Shellshock	Exploit CVE-2014-6271 and setup DNS tunnels to exfiltrate stolen data.	packet loss, get kernel version, access /etc/passwd, excessive DNS reqs.
A7	CPU Bug	Exploit a local privilege escalation vulnerability CVE-2017-5754 to steal source code files and extract passwords in the Firefox browser [72].	Get kernel version, get source code file, compile, excessive POST requests.
A8	VM Escape	Exploit a Virtual Box vulnerability CVE-2018-2676 to control the host machine and extract private GPG keys.	Access mem disk, compile, access secring.gpg, excessive UDP requests.
A9	Race Condition	Exploit a race condition in a digital wallet platform to steal the private key.	High network flows, access privkey.pem, excessive ICMP requests.
A10	Obj Deserialization	Exploit an object deserialization vulnerability in the Python pickle module to steal private TLS keys.	Sensitive commands in HTTP request, access privkey.pem.

system concurrently). Although PULSAR processes events as they arrive, it filters out insignificant events by only adding statistically significant (identified by a low p-value) factor functions. Such filtering significantly reduces the number of events in both our training and testing data. PULSAR filtered this stream of an average of 94,238 events to an average of 1,885 significant events that it performed inference. Thus, PULSAR is robust to spurious or noisy events, e.g., ones triggered by benign user activities.

**Challenge 3.** Malware or malicious traffic can proliferate out of control [73]. To ensure full control over the replayed attack scenarios, we contained each attack in a Linux container and further encapsulated it in a virtual machine with limited capabilities. All containers used in our experiments ran in a network sandbox that implemented a Layer-3 private overlay network on a separated Classless Inter-Domain Routing block.

**Challenge 4.** Reproducing old, vulnerabilities is challenging because new Linux distributions already patch old ones out of the box. For example, to reproduce the Container Escape vulnerability, one would have to obtain not only an old Linux distribution released just before the vulnerability announcement date, but also all dependent package repositories. To address this issue, we built a tool to create old Linux containers at any point in the past (2005–present) using the Debian Linux snapshot repository. This tool allows us to reproduce network-based attack scenarios that include i) a vulnerable server container with an unpatched kernel, user applications, and their dependencies; and ii) an attack container with corresponding exploits (e.g., ICMP tunneling tools). Thus, our approach is more extensible than Metasploit, which only provides exploit code, or a tool introduced in [74], which only provides scenarios for memory error vulnerabilities on the host.

With the above challenges solved, we created a testbed environment for automated replay of APTs in production. The data collected from the replayed APTs were used to measure the accuracy and preemption capabilities of PULSAR.

**Accuracy measurement.** We compared PULSAR’s accuracy in detecting the ten unseen APTs with that of the *event from any monitor (EA)*, *event correlation (EC)*, and *event statistical anomaly (ES)* techniques currently deployed at SystemX. The

*EA* method is a degenerate approach in which every event is declared to be an attack. The *EC* is implemented using Bro and osquery [75]; it relies on i) an extensive signature database aggregated from more than 30 anti-virus vendors [76]) and ii) manually created correlation rules, e.g., a brute-force SSH login followed by a successful root login, based on host/network event types (similar to the alert correlation technique in [77]). The *ES* includes a set of statistical measures (similar to ones in [78], [79]) calculated from the outputs of the deployed security monitors, e.g., days since last login.

**Experiment 3: Performance and accuracy of PULSAR in production at SystemX.** To validate PULSAR’s runtime performance in the production network while real workloads were running, we deployed PULSAR in SystemX for one month and measured its memory consumption, event processing latency, and observed its decisions.

To determine the performance impact of PULSAR on the regular workload, we measured i) runtime memory used by PULSAR, and ii) the latency of PULSAR’s algorithms (implemented as a single but multithreaded process based on a C++ OpenGM framework [80]). All measurements were run in a single 56-core 2 GHz Intel Xeon E5 with 128GB RAM.

## VI. RESULTS

This section presents the results of the experiments above.

**Result 1: Evaluation based on data on successful past APTs.** Fig. 9 shows PULSAR’s attack stage detection accuracy in terms of the *F-measure* of the precision-recall spectra. F-measure is the 2-times harmonic mean of precision and recall, is upper-bounded by 1, and maps directly to the effectiveness of PULSAR, with larger numbers signifying better accuracy. The F-measure range is [63.3%, 98.9%] with an average accuracy of attack stage detection of 93.5%. PULSAR shows lower effectiveness in accurately identifying attack stages corresponding to the attack preparation phase ( $\sigma_6$  was accurately detected only 63.3% of the time). The reason for the lower accuracy is that many events (e.g., download) generated at the preparation stage overlap with legitimate user activities. For example, a code download frequently corresponds to a legitimate user activity). At SystemX, we have observed that 89% of users who perform file downloads are legitimate.

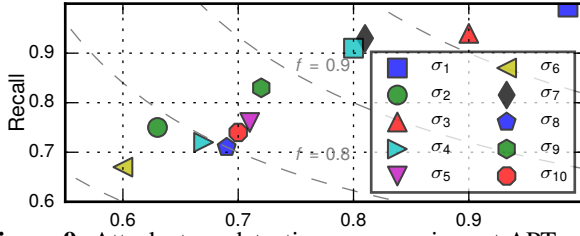


**Figure 9:** Attack stage detection accuracy in past APTs. Dotted contour lines represent the  $F$ -measure of the precision-recall spectra. The majority of detected attack stages are clustered close to  $F$ -measure = 1, i.e., better precision-recall.

Even so, PULSAR detected 55 out of 60 attacks and performed the best in detecting the benign stage  $\sigma_0$  (which it did 98.9% of the time with a low FPR) and the gathering stage  $\sigma_3$  (which it did 92.0% of the time – showing that it could preempt attacks before system integrity violation).

**Result 2: Evaluation based on data on ten unseen attacks injected in live traffic at SystemX.** PULSAR’s accuracy in detecting attack stages in the ten unseen attacks is quantified in Fig. 10 in comparison with the three methods (described in §V) currently deployed in SystemX. First, we studied the true-positive rate (TPR), which is representative of the overall accuracy of the PULSAR system in correctly identifying APTs. Fig. 10 shows that PULSAR significantly outperforms the EC and ES techniques (§V). The TPR for PULSAR is 84.8%, while it is 18.4% and 11.4% for EC and ES, respectively. The EA has 100% accuracy because it indicates an APT for any observed event. Second, we studied the false-positive rate (FPR) which was representative of the number of events generated by legitimate users but detected as attacks. The FPR is important from a security administrator perspective, as a high FPR can overwhelm a human operator’s ability to react to an attack quickly. We observe (from Fig. 10) that the EC offers a near-zero FPR (which is expected, because EC matches specific event patterns) and that the ES performs poorly on the FPR (the EA has a 99.7% FPR because all events, including ones from legitimate users, are considered attacks). PULSAR’s small but non-zero FPR (0.02%) can be attributed to production traffic that interleaves with attack-related activities when we replay a given attack. This traffic adds noise to the stream of events observed by PULSAR. In the context of TPR and FPR, PULSAR offers a trade-off between high attack detection accuracy and a low FPR.

PULSAR preempts attacks and does not need to be informed by monitors of severe events (at the end of attacks). Table V summarizes the effectiveness of the four methods (compared in this analysis) in terms of two metrics: (i) preemption of system integrity violation and data loss (SI+DL) and (ii) preemption of data loss while allowing integrity violation (DL). The third column in Table V shows the median number of stages (hops) that each method is able to detect the attack before system integrity violation. The last column in Table V shows the FPR when we evaluated PULSAR on ten unseen scenarios ran in live production traffic that produced a total of 1.25M events (Table III). The EC has a low FPR (0.051%), however, it preempts only one attack out of ten before system integrity violation. Although PULSAR could not stop all system integrity violations, it was able to stop eight attacks out of ten at least

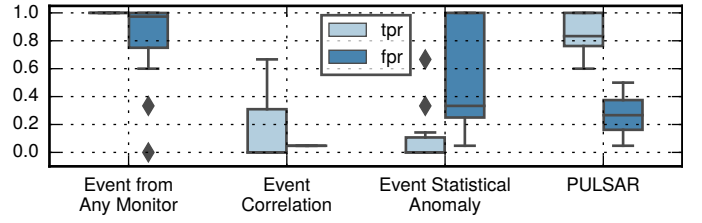


**Figure 10:** TPR and FPR of the techniques across attack stages. The boxes represent quartiles; the notch represents the median, and the whiskers represent the maximum and minimum.

**Table V:** Summary of an early detection result for ten attacks

Method	Median hop	SI+DL	DL	False Positive
EA	4	10	10	99.706%
EC	1	1	2	00.051%
ES	0	0	3	00.040%
<b>PULSAR</b>	<b>3</b>	<b>8</b>	<b>10</b>	<b>00.020%</b>

SI: System integrity violation; DL: Data loss

SI+DL: Attacks stopped before SI and DL

DL: Attacks stopped after SI but before DL

one hop before system integrity violation without needing to observe of any critical event (e.g., installation of a kernel module) from underlying monitors. In addition, PULSAR stopped all ten attacks up to three stages (in the median case) before data loss. PULSAR has the lowest FPR (i.e., fraction of events incorrectly classified as attacks), 0.020%, which is 2× better than that of the second-best method (i.e., 0.040% in ES).

**Result 3: Evaluation based on data from PULSAR deployment in the production SystemX.** A key performance metric for characterizing PULSAR deployment in the production environment is the observed FPR, in terms of both the percentage and the absolute number of false alerts [7]. Given increasing amounts of network traffic and host activities, even a small FPR can quickly overwhelm a security analyst’s ability to react to an attack. We tested PULSAR in a production environment in which attack traffic was naturally interleaved with legitimate user activities, i.e., background network traffic and host activities, making detection significantly more difficult. Table VI shows the list of the top 5 most/least frequent events. Even under those noisy operational conditions, PULSAR had an impressive FPR of 0.009%, which corresponds to an average of nine false detections out of an average of 94K daily events. Three out of nine false detections were correlated with three known malicious downloads (shown in Table VI), in which malicious files (e.g., discussed in [81], [82]) were downloaded because of user mistakes, but none of those malicious files was executed. The remaining six out of nine false detections were related to Apache Struts exploit attempts followed by unusual host activities (e.g., disabling of Bash history logging).

**Runtime Performance.** Since SystemX has hundreds of active users a day, we configured PULSAR to handle at most 1,000 concurrent users with a sliding window size of 10,000 events per user. The window size must be long enough to accommodate long-duration APTs [5]. In this configuration, PULSAR can handle events for APTs that last up to 217 days ( $10,000 \text{ events} / 46 \text{ events per day for a user}$ ), assuming 46 events per user per day as calculated in §V. PULSAR takes a median of 1.06 seconds (variance = 0.03) from observing an event to

**Table VI:** Listing of top 5 most frequent and least frequent alerts during a one-month deployment in production (2018).

Count	Service	Name	Description/Example
145.9K	SSH	Subnet_Scanner	Scan for SSH hosts
133.8K	SSL	Invalid_Cert	Invalid server certificate
23.4K	HTTP	Struts	Exploit Apache Struts
1.9K	DNS	Excessive	Large outgoing DNS requests
1.8K	HTTP	Shellshock	Attempt to exploit Bash
175	RDP	Brute Force	Remote desktop login
93	ARP	Unknown_Host	New host on internal network
39	HTTP	Exposed	An internal server is exposed
36	HTTP	SQL_Injection	Inject SQL commands
3	HTTP	Bad_Download	A known malicious file

making a decision (Fig. 11), which is well within the 31-minute inter-event arrival rate of events for each user in SystemX (as calculated in §V). PULSAR requires only 126MiB of memory for each monitored user (i.e., 126GiB of memory for the production deployment of 1,000 users; see Fig. 11).

The PULSAR algorithm’s scales as  $O(n)$ , where  $n$  the number of nodes (which includes the numbers of observed events, unknown states, and actions) and the number of FFs (which is fixed from the training data and does not change at runtime) in the graph [33]. PULSAR is currently implemented as a single process, and this limits the number of users that PULSAR can handle at the same time (1000). PULSAR can leverage [83] to scale to a larger number of users.

## VII. DISCUSSION

**Explaining PULSAR’s success.** As we pointed out in our threat model (§III), the success of our approach depends on some overlaps between unseen APTs and past APTs. As we have shown in our results (§VI), PULSAR has learned prior knowledge (in terms of commonality, severity, and repetitiveness FFs) from a broad set of 120 past APTs. In fact, each unseen attack (in our ten scenarios shown in Table IV) has an average of six key events (not counting excessive scan events) out of a maximum of 30 events and a minimum of 12 events that are common with past APTs. This relatively modest level of similarity with past events enables PULSAR to detect unseen attacks. It is important to note that the training data had only thousands of events, while PULSAR in production observed millions of background events. This means the number of attacks (albeit many unsuccessful) has increased significantly.

**Generalizing PULSAR trained knowledge to other systems.** A pre-trained instance of PULSAR (e.g., based on data from SystemX) can be ported to another system under two assumptions: the new system uses industry-standard monitors such as Bro to output events that have the same semantics as in  $\mathcal{E}$  and a similar number of users. The assumptions reflect a limitation of the current PULSAR implementation, not its inference algorithm. While a new environment might have new events that are not in our defined event set  $\mathcal{E}$ , incorporating such new events into PULSAR would not require a retraining of the old FFs. Instead, only new FFs that are related to the new events need to be learned and used for inference.

## VIII. RELATED WORK

The signature-based techniques (SBTs) [6], [10], [84]–[87] identify specific hashes of attack payloads. Hence, they are suitable only for identifying a specific stage of an attack (such as the use of a known rootkit at a late attack stage). They are not suitable for preemptive detection of APTs because each

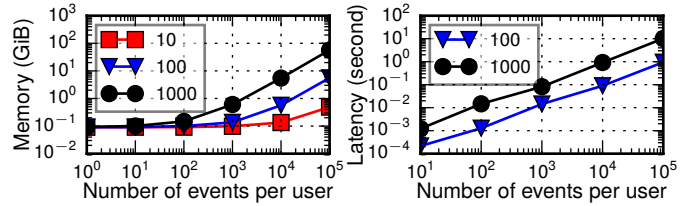


**Figure 11:** Memory and latency performance of PULSAR for 10,100,1000 users with a varying size of window of events.

stage may look benign when analyzed in isolation, but together they show malicious intent (e.g., see §II-C). The anomaly-based techniques (ABTs) [19], [20], [88]–[102] construct a normal usage profile from past training data and measure a statistical distance to find anomalous usage profiles at runtime. As a result, potentially novel attacks can be captured, but at the cost of a high number of false detection [103]. Thus, security operators must select anomaly features carefully.

Detection models based on PGMs [104]–[107] have been built based on expert-defined libraries of known attacks. Thus, the detection accuracy is often proportional to the manual work involved in creating features. *Alert correlation* [75], [77] and *data provenance* [108], [109] techniques combine related events of the same attack instance into a stream of events. However, for large-scale systems, hundreds of events occur concurrently, so simply filtering and ordering events do not work. *Attack graph* techniques [110]–[115] illustrate possible attack scenarios, so they are useful for system administrators in deploying appropriate security monitors to defend their systems. The common problem across ML techniques [112], [116]–[119], however, is that they have been trained on outdated [120] or synthetic datasets that contain artificial background traffic. Some attack detection techniques in [19], [121] only consider host-level events. Forensic analyses [122]–[130] localize compromised hosts post-incident, e.g., using post-compromise communication traces [131], therefore, they are not suitable for preemptive detection. Overall, it is unclear whether these solutions can be successful in preempting APTs.

Applying ML and security presents several challenges [132]. First, while some ML models offer low FPR (e.g., 0.1%), these models suffer from high FPR for large-scale deployment (e.g., a million security events per day  $\times$  0.1% = 1,000 false alerts per day). PULSAR lowers the FPR by only using statistically significance FFs learned from our real-world study of 120 APTs, thus compensating for the shortcomings of IDSs [133]. In the future, it will likely be beneficial to deploy PULSAR on smart IDSs [134]. Second, while existing work uses outdated [120], [135], short-term [136], or limited variety of attack type datasets [137], [138], our source training data are longitudinal (representing 10-year) and have been collected in real production traffic with up-to-date attack activities (until 2018). Third, while deep-learning models, e.g., [90], are promising, they offer analysts few explanations on how the models work. In contrast, PULSAR clearly shows the evolution of each attack stage; thereby enabling APTs response.

## IX. CONCLUSION

This paper presented PULSAR, a preemptive intrusion detection and response framework for the detection of Advanced Persistent Threats. PULSAR has been deployed at SystemX and demonstrated accurate attack preemption with a low FPR.



## REFERENCES

- [1] “Glossary of key information security terms,” *NIST*, 2018, <https://csrc.nist.gov/glossary/term/advanced-persistent-threat>.
- [2] “Ibm x-force threat intelligence,” 2017, <https://ibm.com/security/xforce>. [Online]. Available: <https://ibm.com/security/xforce>
- [3] “Adversarial tactics, techniques and common knowledge,” 2017, [https://attack.mitre.org/wiki/Main\\_Page](https://attack.mitre.org/wiki/Main_Page). [Online]. Available: [https://attack.mitre.org/wiki/Main\\_Page](https://attack.mitre.org/wiki/Main_Page)
- [4] T. Lauinger et al., “Thou shalt not depend on me: Analysing the use of outdated javascript libraries on the web,” in *NDSS*, 2017.
- [5] “Apt notes,” *Github*, 2017, <https://github.com/aptnotes/data/blob/master/APTnotes.csv>.
- [6] “The bro network security monitor,” 2018, <https://bro.org>.
- [7] S. Axelsson, “The base-rate fallacy and its implications for the difficulty of intrusion detection,” in *Proc 6th ACM Conf on Computer and Communications Security*, 1999, pp. 1–7.
- [8] T. Basso et al., “Analysis of the effect of java software faults on security vulnerabilities and their detection by commercial web vulnerability scanner tool,” in *Dependable Systems and Networks Workshops (DSN-W), 2010 International Conference on*. IEEE, 2010, pp. 150–155.
- [9] M. Roesch et al., “Snort: Lightweight intrusion detection for networks,” in *Lisa*, vol. 99, no. 1, 1999, pp. 229–238.
- [10] *osquery*. Facebook, 2018, <https://osquery.io/>.
- [11] “Equifax: Cybersecurity incident and important consumer information,” 2017, <https://investor.equifax.com/news-and-events/news/2017/09-15-2017-224018832>. [Online]. Available: <https://investor.equifax.com/news-and-events/news/2017/09-15-2017-224018832>
- [12] D. Muthukumaran et al., “Flowwatcher: Defending against data disclosure vulnerabilities in web applications,” in *Proceedings of the 22nd ACM SIGSAC Conference on Computer and Communications Security*. ACM, 2015, pp. 603–615.
- [13] A. D’Amico and K. Whitley, “The real work of computer network defense analysts,” in *ViSEC 2007*. Springer, 2008, pp. 19–37.
- [14] A. M. Bates et al., “Trustworthy whole-system provenance for the linux kernel,” in *USENIX Security Symposium*, 2015, pp. 319–334.
- [15] W. U. Hassan et al., “Nodoze: Combatting threat alert fatigue with automated provenance triage,”
- [16] Y. Cao et al., “Abusing browser address bar for fun and profit—an empirical investigation of add-on cross site scripting attacks,” in *International Conference on Security and Privacy in Communication Systems*. Springer, 2014, pp. 582–601.
- [17] D. Cotroneo, A. Paudice, and A. Pecchia, “Automated root cause identification of security alerts: Evaluation in a saas cloud,” *Future Generation Computer Systems*, vol. 56, pp. 375–387, 2016.
- [18] A. Paudice, S. Sarkar, and D. Cotroneo, “An experiment with conceptual clustering for the analysis of security alerts,” in *Software Reliability Engineering Workshops (ISSREW), 2014 IEEE International Symposium on*. IEEE, 2014, pp. 335–340.
- [19] K. Xu et al., “A sharper sense of self: Probabilistic reasoning of program behaviors for anomaly detection with context sensitivity,” in *Dependable Systems and Networks (DSN), 2016 46th Annual IEEE/IFIP Intl. Conf on*. IEEE, 2016, pp. 467–478.
- [20] T.-F. Yen et al., “Beehive: Large-scale log analysis for detecting suspicious activity in enterprise networks,” in *Proc 29th Annual Computer Security Applications Conf*. ACM, 2013, pp. 199–208.
- [21] T. Shon et al., “A machine learning framework for network anomaly detection using svm and ga,” in *Information Assurance Workshop, 2005. IAW’05. Proceedings from the Sixth Annual IEEE SMC*. IEEE, 2005, pp. 176–183.
- [22] S. M. Milajerdi et al., “Holmes: Real-time apt detection through correlation of suspicious information flows,” in *HOLMES: Real-Time APT Detection through Correlation of Suspicious Information Flows*. IEEE, p. 0.
- [23] E. C. Badger, “Scalable data analytics pipeline for real-time attack detection: design, validation, and deployment in a honeypot environment,” 2015.
- [24] R. Talbi, S. Bouchenak, and L. Y. Chen, “Towards dynamic end-to-end privacy preserving data classification,” in *2018 48th Annual IEEE/IFIP International Conference on Dependable Systems and Networks Workshops (DSN-W)*. IEEE, 2018, pp. 73–74.
- [25] H.-L. Chen et al., “Evaluating the risk of data disclosure using noise estimation for differential privacy,” in *Dependable Computing (PRDC), 2017 IEEE 22nd Pacific Rim International Symposium on*. IEEE, 2017, pp. 339–347.
- [26] D. R. Karger, S. Oh, and D. Shah, “Iterative learning for reliable crowdsourcing systems,” in *Advances in neural information processing systems*, 2011, pp. 1953–1961.
- [27] A. Ratner et al., “Snorkel: Rapid training data creation with weak supervision,” *Proceedings of the VLDB Endowment*, vol. 11, no. 3, pp. 269–282, 2017.
- [28] T. Bonaci et al., “Experimental analysis of denial-of-service attacks on teleoperated robotic systems,” in *Proceedings of the ACM/IEEE Sixth International Conference on Cyber-Physical Systems*. ACM, 2015, pp. 11–20.
- [29] “Nist data structures,” 2014, <https://linux.nist.gov/dads/HTML/longestCommonSubsequence.html>. [Online]. Available: <https://linux.nist.gov/dads/HTML/longestCommonSubsequence.html>
- [30] “Cve-2017-5638,” <https://nvd.nist.gov/vuln/detail/CVE-2017-5638>.
- [31] “Cve-2016-5195,” <https://nvd.nist.gov/vuln/detail/CVE-2016-5195>.
- [32] M. Beccuti et al., “Markov decision petri nets with uncertainty,” in *European Workshop on Performance Engineering*. Springer, 2015, pp. 177–192.
- [33] B. J. Frey et al., “Factor graphs and algorithms,” in *Proc Annual Allerton Conf on Communication Control and Computing*, vol. 35. UNIVERSITY OF ILLINOIS, 1997, pp. 666–680.
- [34] J. Pearl, “Bayesian networks,” 2011.
- [35] W. H. Sanders and J. F. Meyer, “Metasan: A performability evaluation tool based on stochastic activity networks,” in *Proceedings of 1986 ACM Fall joint computer conference*. IEEE Computer Society Press, 1986, pp. 807–816.
- [36] M. Halkidi et al., “Resilient and energy efficient tracking in sensor networks,” *International Journal of Wireless and Mobile Computing*, vol. 1, no. 2, pp. 87–100, 2006.
- [37] V. Kulkarni et al., “On the inability of markov models to capture criticality in human mobility,” *arXiv preprint arXiv:1807.11386*, 2018.
- [38] K. R. Joshi et al., “Probabilistic model-driven recovery in distributed systems,” *IEEE Transactions on Dependable and Secure Computing*, vol. 8, no. 6, pp. 913–928, 2011.
- [39] R. Skowrya et al., “Effective topology tampering attacks and defenses in software-defined networks,” in *2018 48th Annual IEEE/IFIP International Conference on Dependable Systems and Networks (DSN)*. IEEE, 2018, pp. 374–385.
- [40] B. E. Ujich, U. Thakore, and W. H. Sanders, “Attain: An attack injection framework for software-defined networking,” in *Dependable Systems and Networks (DSN), 2017 47th Annual IEEE/IFIP International Conference on*. IEEE, 2017, pp. 567–578.
- [41] H. Wang, L. Xu, and G. Gu, “Floodguard: A dos attack prevention extension in software-defined networks,” in *2015 45th Annual IEEE/IFIP International Conference on Dependable Systems and Networks*. IEEE, 2015, pp. 239–250.
- [42] S. Zhang et al., “An adaptable rule placement for software-defined networks,” in *Dependable Systems and Networks (DSN), 2014 44th Annual IEEE/IFIP International Conference on*. IEEE, 2014, pp. 88–99.
- [43] H. Truta et al., “A predictive approach for enhancing resource utilization in paas clouds,” in *Proceedings of the Symposium on Applied Computing*. ACM, 2017, pp. 384–391.
- [44] I. Paschenko et al., “Vulnerable open source dependencies: Counting those that matter,” in *Proceedings of the 12th International Symposium on Empirical Software Engineering and Measurement (ESEM)*, Oct 2018.
- [45] T. Lauinger et al., “Thou shalt not depend on me: Analysing the use of outdated javascript libraries on the web,” in *Proceedings of NDSS*, 2017.
- [46] M. Garcia et al., “Os diversity for intrusion tolerance: Myth or reality?” in *Dependable Systems & Networks (DSN), 2011 IEEE/IFIP 41st International Conference on*. IEEE, 2011, pp. 383–394.
- [47] M. Beham, M. Vlad, and H. P. Reiser, “Intrusion detection and honeypots in nested virtualization environments,” in *Dependable Systems and Networks (DSN), 2013 43rd Annual IEEE/IFIP International Conference on*. IEEE, 2013, pp. 1–6.
- [48] A. Babay et al., “Network-attack-resilient intrusion-tolerant scada for the power grid.”
- [49] Y. Liu et al., “Towards a timely causality analysis for enterprise security,” *NDSS*, 2018.
- [50] S. T. King et al., “Enriching intrusion alerts through multi-host causality,” in *NDSS*, 2005.
- [51] K. H. Lee, X. Zhang, and D. Xu, “High accuracy attack provenance via binary-based execution partition,” in *NDSS*, 2013.
- [52] S. Ma, X. Zhang, and D. Xu, “Protracer: Towards practical provenance tracing by alternating between logging and tainting,” in *NDSS*, 2016.
- [53] Y. Xia et al., “Cfimon: Detecting violation of control flow integrity using performance counters,” in *Dependable Systems and Networks (DSN), 2012 42nd Annual IEEE/IFIP International Conference on*. IEEE, 2012, pp. 1–12.
- [54] A. Kurmus, A. Sornioti, and R. Kapitza, “Attack surface reduction for commodity os kernels: trimmed garden plants may attract less bugs,” in *Proceedings of the Fourth European Workshop on System Security*. ACM, 2011, p. 6.
- [55] S. Hossain et al., “Towards cyber-physical intrusion tolerance,” in *Smart Grid Communications (SmartGridComm), 2015 IEEE International Conference on*. IEEE, 2015, pp. 139–144.
- [56] M. L. Mazurek et al., “Measuring password guessability for an entire university,” in *Proc 2013 ACM SIGSAC conference on Computer & communications security*. ACM, 2013, pp. 173–186.
- [57] M. Egele et al., “Towards detecting compromised accounts on social networks,” *IEEE Trans Dependable and Secure Computing*, vol. 14, no. 4, pp. 447–460, 2017.
- [58] T. Barron and N. Nikiforakis, “Picky attackers: Quantifying the role of system properties on intruder behavior,” in *Proc 33rd Annual Computer Security Applications Conf. ser. ACSAC 2017, 2017*, pp. 387–398.
- [59] W. Han et al., “Shadow attacks based on password reuses: A quantitative empirical view,” *IEEE Trans Dependable and Secure Computing*, 2016.
- [60] D. Wagner and P. Soto, “Mimicry attacks on host-based intrusion detection systems,” in *Proceedings of the 9th ACM Conference on Computer and Communications Security*. ACM, 2002, pp. 255–264.
- [61] “ph: Process homeostasis,” <http://people.scs.carleton.ca/~mvvelzen/pH/pH.html>, 2008.
- [62] D. J. Sheskin, *Handbook of parametric and nonparametric statistical procedures*. crc Press, 2003.
- [63] M. J. Atallah, *Algorithms and theory of computation handbook*. CRC press, 1998.
- [64] B. J. Kwon et al., “Catching worms, trojan horses and pups: Unsupervised detection of silent delivery campaigns,” *arXiv preprint arXiv:1611.02787*, 2016.
- [65] A. Doupé et al., “Enemy of the state: A state-aware black-box web vulnerability scanner,” in *USENIX Security Symposium*, vol. 14, 2012.
- [66] N. Schagen et al., “Towards automated vulnerability scanning of network servers,” in *Proc 11th European Workshop on Systems Security*. ACM, 2018, p. 5.
- [67] J. S. Yedidia, W. T. Freeman, and Y. Weiss, “Constructing free-energy approximations and generalized belief propagation algorithms,” *IEEE Trans information theory*, vol. 51, no. 7, pp. 2282–2312, 2005.
- [68] V. Kolmogorov, “Convergent tree-reweighted message passing for energy minimization,” *IEEE transactions on pattern analysis and machine intelligence*, vol. 28, no. 10, pp. 1568–1583, 2006.
- [69] M. Erdt, A. Fernández, and C. Rensing, “Evaluating recommender systems for technology enhanced learning: a quantitative survey,” *IEEE Transactions on Learning Technologies*, vol. 8, no. 4, pp. 326–344, 2015.
- [70] “Facebook security breach exposes 50 million user account,” *NYTIMES*, 2018, <https://newsroom.fb.com/news/2018/10/update-on-security-issue/>.
- [71] “Cve-2017-1000433,” <https://nvd.nist.gov/vuln/detail/CVE-2017-1000433>.
- [72] M. Lipp et al., “Meltdown: Reading kernel memory from user space,” 2018.

- [73] X. Gao *et al.*, "Containerleaks: emerging security threats of information leakages in container clouds," in *Dependable Systems and Networks (DSN), 2017 47th Annual IEEE/IFIP International Conference on*. IEEE, 2017, pp. 237–248.
- [74] D. Mu *et al.*, "Understanding the reproducibility of crowd-reported security vulnerabilities," in *USENIX*, 2018.
- [75] "Bro integration with osquery," 2018, <https://github.com/bro/bro-osquery>.
- [76] "The malware hash registry project," 2017, <http://www.team-cymru.org/MHR.html>. [Online]. Available: <http://www.team-cymru.org/MHR.html>
- [77] F. Valeur *et al.*, "Comprehensive approach to intrusion detection alert correlation," *IEEE Trans dependable and secure computing*, vol. 1, no. 3, pp. 146–169, 2004.
- [78] D. Freeman *et al.*, "Who are you? a statistical approach to measuring user authenticity," in *NDSS*, 2016, pp. 1–15.
- [79] E. C. Ngai, J. Liu, and M. R. Lyu, "An efficient intruder detection algorithm against sinkhole attacks in wireless sensor networks," *Computer Communications*, vol. 30, no. 11–12, pp. 2353–2364, 2007.
- [80] B. Andres, T. Beier, and J. H. Kappes, "Opengm: A c++ library for discrete graphical models," *arXiv preprint arXiv:1206.0111*, 2012.
- [81] B. Rahbarinia, M. Balduzzi, and R. Perdisci, "Exploring the long tail of (malicious) software downloads," in *2017 47th Annual IEEE/IFIP International Conference on Dependable Systems and Networks (DSN)*. IEEE, 2017, pp. 391–402.
- [82] B. Stock, B. Livshits, and B. Zorn, "Kizzle: a signature compiler for detecting exploit kits," in *Dependable Systems and Networks (DSN), 2016 46th Annual IEEE/IFIP International Conference on*. IEEE, 2016, pp. 455–466.
- [83] M. Zaharia *et al.*, "Apache spark: a unified engine for big data processing," *Communications of the ACM*, vol. 59, no. 11, pp. 56–65, 2016.
- [84] M. Egele *et al.*, "Using static program analysis to aid intrusion detection," in *Intl. Conf on Detection of Intrusions and Malware, and Vulnerability Assessment*. Springer, 2006, pp. 17–36.
- [85] M. Shimamura and K. Kono, "Using attack information to reduce false positives in network ids," in *Computers and Communications, 2006. ISCC'06. Proceedings. 11th IEEE Symposium on*. IEEE, 2006, pp. 386–393.
- [86] F. Massicotte and Y. Labiche, "An analysis of signature overlaps in intrusion detection systems," in *Dependable Systems & Networks (DSN), 2011 IEEE/IFIP 41st International Conference on*. IEEE, 2011, pp. 109–120.
- [87] S. Zhao *et al.*, "Owl: Understanding and detecting concurrency attacks."
- [88] S.-Y. Huang and Y.-N. Huang, "Network traffic anomaly detection based on growing hierarchical som," in *Dependable Systems and Networks (DSN), 2013 43rd Annual IEEE/IFIP International Conference on*. IEEE, 2013, pp. 1–2.
- [89] E. Anceaume *et al.*, "Anomaly characterization in large scale networks," in *Dependable Systems and Networks (DSN), 2014 44th Annual IEEE/IFIP International Conference on*. IEEE, 2014, pp. 68–79.
- [90] M. Du *et al.*, "Deeplog: Anomaly detection and diagnosis from system logs through deep learning," in *Proc 2017 ACM SIGSAC Conf on Computer and Communications Security*. ACM, 2017, pp. 1285–1298.
- [91] X. Shu, D. D. Yao, and B. G. Ryder, "A formal framework for program anomaly detection," in *Intl. Workshop on Recent Advances in Intrusion Detection*. Springer, 2015, pp. 270–292.
- [92] A. P. Athreya *et al.*, "Poster: Packet conductance for statistical intrusion detection in anonymous networks."
- [93] M. Le, A. Stavrou, and B. B. Kang, "Doubleguard: Detecting intrusions in multitier web applications," *IEEE Trans dependable and secure computing*, vol. 9, no. 4, pp. 512–525, 2012.
- [94] J. Chu *et al.*, "Alert-id: Analyze logs of the network element in real time for intrusion detection," in *International Workshop on Recent Advances in Intrusion Detection*. Springer, 2012, pp. 294–313.
- [95] A. Dhakal and K. Ramakrishnan, "Machine learning at the network edge for automated home intrusion monitoring," in *Network Protocols (ICNP), 2017 IEEE 25th International Conference on*. IEEE, 2017, pp. 1–6.
- [96] T. Zoppi, A. Ceccarelli, and A. Bondavalli, "Context-awareness to improve anomaly detection in dynamic service oriented architectures," in *International Conference on Computer Safety, Reliability, and Security*. Springer, 2016, pp. 145–158.
- [97] M. Vadursi *et al.*, "System and network security: anomaly detection and monitoring," *Journal of Electrical and Computer Engineering*, vol. 2016, 2016.
- [98] M. Cinque, R. Della Corte, and A. Pecchia, "Entropy-based security analytics: Measurements from a critical information system," in *Dependable Systems and Networks (DSN), 2017 47th Annual IEEE/IFIP International Conference on*. IEEE, 2017, pp. 379–390.
- [99] C. Feng, T. Li, and D. Chana, "Multi-level anomaly detection in industrial control systems via package signatures and lstm networks," in *Dependable Systems and Networks (DSN), 2017 47th Annual IEEE/IFIP International Conference on*. IEEE, 2017, pp. 261–272.
- [100] S. Lee *et al.*, "Athena: A framework for scalable anomaly detection in software-defined networks," in *2017 47th Annual IEEE/IFIP International Conference on Dependable Systems and Networks (DSN)*. IEEE, 2017, pp. 249–260.
- [101] J. Zhang *et al.*, "Detecting stealthy p2p botnets using statistical traffic fingerprints," 2011.
- [102] V. Narayanan and R. B. Bobba, "Learning based anomaly detection for industrial arm applications," in *Proceedings of the 2018 Workshop on Cyber-Physical Systems Security and Privacy*. ACM, 2018, pp. 13–23.
- [103] C. Gates and C. Taylor, "Challenging the anomaly detection paradigm: a provocative discussion," in *Proc 2006 workshop on New security paradigms*. ACM, 2006, pp. 21–29.
- [104] P. Holgado, V. A. VILLAGRA, and L. Vazquez, "Real-time multistep attack prediction based on hidden markov models," *IEEE Trans Dependable and Secure Computing*, 2017.
- [105] P. Ning and D. Xu, "Learning attack strategies from intrusion alerts," in *Proc 10th ACM conference on Computer and communications security*. ACM, 2003, pp. 200–209.
- [106] "Teddi: Tamper event detection on distributed cyber-physical systems," 2016, <https://cs.dartmouth.edu/trdata/TR2016-804.pdf>. [Online]. Available: <https://www.cs.dartmouth.edu/~trdata/reports/TR2016-804.pdf>
- [107] P. Cao *et al.*, "Preemptive intrusion detection: Theoretical framework and real-world measurements," in *Proc 2015 Symposium and Bootcamp on the Science of Security*. ACM, 2015, p. 5.
- [108] Y. Ji *et al.*, "Rain: Refinable attack investigation with on-demand inter-process information flow tracking," in *Proc 2017 ACM SIGSAC Conf on Computer and Communications Security*. ACM, 2017, pp. 377–390.
- [109] W. U. Hassan *et al.*, "Towards scalable cluster auditing through grammatical inference over provenance graphs."
- [110] M. Albanese, S. Jajodia, and S. Noel, "Time-efficient and cost-effective network hardening using attack graphs," in *Dependable Systems and Networks (DSN), 2012 42nd Annual IEEE/IFIP International Conference on*. IEEE, 2012, pp. 1–12.
- [111] O. Sheyner and J. Wing, "Tools for generating and analyzing attack graphs," in *Intl. Symposium on Formal Methods for Components and Objects*. Springer, 2003, pp. 344–371.
- [112] L. Ravindranath *et al.*, "Change is hard: adapting dependency graph models for unified diagnosis in wired/wireless networks," in *Proceedings of the 1st ACM workshop on Research on enterprise networking*. ACM, 2009, pp. 83–92.
- [113] N. Nostro *et al.*, "On security countermeasures ranking through threat analysis," in *International Conference on Computer Safety, Reliability, and Security*. Springer, 2014, pp. 243–254.
- [114] R. Han *et al.*, "Work-in-progress: Maximizing model accuracy in real-time and iterative machine learning," in *Real-Time Systems Symposium (RTSS), 2017 IEEE*. IEEE, 2017, pp. 351–353.
- [115] D. Didona and P. Romano, "Using analytical models to bootstrap machine learning performance predictors," in *Parallel and Distributed Systems (ICPADS), 2015 IEEE 21st International Conference on*. IEEE, 2015, pp. 405–413.
- [116] P. Xie *et al.*, "Using bayesian networks for cyber security analysis," in *Dependable Systems and Networks (DSN), 2010 IEEE/IFIP international conference on*. IEEE, 2010, pp. 211–220.
- [117] J. McHugh, "Testing intrusion detection systems: A critique of the 1998 and 1999 darpa intrusion detection system evaluations as performed by lincoln laboratory," *ACM Trans. Inf. Syst. Secur.*, vol. 3, no. 4, pp. 262–294, Nov. 2000.
- [118] H. Du and S. J. Yang, "Probabilistic inference for obfuscated network attack sequences," in *Dependable Systems and Networks (DSN), 2014 44th Annual IEEE/IFIP International Conference on*. IEEE, 2014, pp. 57–67.
- [119] J. Lee and G. de Veciana, "Scalable multicast based filtering and tracing framework for defeating distributed dos attacks," *International Journal of Network Management*, vol. 15, no. 1, pp. 43–60, 2005.
- [120] "Darpa intrusion detection data sets," 1999, <https://www.ll.mit.edu/ideval/data/>. [Online]. Available: <https://www.ll.mit.edu/ideval/data/>
- [121] S. Zhao *et al.*, "Owl: Understanding and detecting concurrency attacks," in *2018 48th Annual IEEE/IFIP International Conference on Dependable Systems and Networks (DSN)*. IEEE, 2018, pp. 219–230.
- [122] A. Houmansadr, S. A. Zonouz, and R. Berthier, "A cloud-based intrusion detection and response system for mobile phones," in *Dependable Systems and Networks Workshops (DSN-W), 2011 IEEE/IFIP 41st Intl. Conf on*. IEEE, 2011, pp. 31–32.
- [123] A. Pecchia *et al.*, "Identifying compromised users in shared computing infrastructures: A data-driven bayesian network approach," in *Reliable Distributed Systems (SRDS), 2011 30th IEEE Symposium on*. IEEE, 2011, pp. 127–136.
- [124] K. Pei *et al.*, "Hercule: attack story reconstruction via community discovery on correlated log graph," in *Proc 32nd Annual Conf on Computer Security Applications*. ACM, 2016, pp. 583–595.
- [125] T.-F. Yen *et al.*, "An epidemiological study of malware encounters in a large enterprise," in *Proc 2014 ACM SIGSAC Conf on Computer and Communications Security*. ACM, 2014, pp. 1117–1130.
- [126] P. Vadev *et al.*, "Enabling reconstruction of attacks on users via efficient browsing snapshots," 2017.
- [127] R. Perdisci, G. Giacinto, and F. Roli, "Alarm clustering for intrusion detection systems in computer networks," *Engineering Applications of Artificial Intelligence*, vol. 19, no. 4, pp. 429–438, 2006.
- [128] X. Hu *et al.*, "Baywatch: Robust beaconing detection to identify infected hosts in large-scale enterprise networks," in *Dependable Systems and Networks (DSN), 2016 46th Annual IEEE/IFIP International Conference on*. IEEE, 2016, pp. 479–490.
- [129] L. Yu *et al.*, "Filtering log data: Finding the needles in the haystack," in *Dependable Systems and Networks (DSN), 2012 42nd Annual IEEE/IFIP International Conference on*. IEEE, 2012, pp. 1–12.
- [130] R. Akrouf *et al.*, "An automated black box approach for web vulnerability identification and attack scenario generation," *Journal of the Brazilian Computer Society*, vol. 20, no. 1, p. 4, 2014.
- [131] A. Oprea *et al.*, "Detection of early-stage enterprise infection by mining large-scale log data," in *Dependable Systems and Networks (DSN), 2015 45th Annual IEEE/IFIP Intl. Conf on*. IEEE, 2015, pp. 45–56.
- [132] R. Sommer and V. Paxson, "Outside the closed world: On using machine learning for network intrusion detection," in *Security and Privacy (SP), 2010 IEEE Symposium on*. IEEE, 2010, pp. 305–316.
- [133] K. Demir and N. Suri, "Towards ddos attack resilient wide area monitoring systems," in *Proceedings of the 12th International Conference on Availability, Reliability and Security*. ACM, 2017, p. 99.
- [134] S. A. Zonouz, K. R. Joshi, and W. H. Sanders, "Cost-aware systemwide intrusion defense via online forensics and on-demand detector deployment," in *Proceedings of the 3rd ACM workshop on Assurable and usable security configuration*. ACM, 2010, pp. 71–74.
- [135] A. Özgür and H. Erdem, "A review of kdd99 dataset usage in intrusion detection and machine learning between 2010 and 2015," *PeerJ PrePrints*, vol. 4, p. e1954v1.
- [136] B. Eshete *et al.*, "Attack analysis results for adversarial engagement 1 of the DARPA transparent computing program," *CoRR*, vol. abs/1610.06936, 2016. [Online]. Available: <http://arxiv.org/abs/1610.06936>

- [137] A. Algaith *et al.*, “Diversity with intrusion detection systems: An empirical study,” in *Network Computing and Applications (NCA), 2017 IEEE 16th International Symposium on*. IEEE, 2017, pp. 1–5.
- [138] A. Gouveia and M. Correia, “A systematic approach for the application of restricted boltzmann machines in network intrusion detection,” in *International Work-Conference on Artificial Neural Networks*. Springer, 2017, pp. 432–446.